

## A model-based approach for filtering magnetic pitch angles obtained by the Motional Stark Effect diagnostic

M.C.C Messmer<sup>1</sup>, F. Felici<sup>1</sup>, J. Loenen<sup>1</sup>, R.J.E. Jaspers<sup>1,2</sup>, M. Reich<sup>3</sup>,

the ASDEX-Upgrade Team<sup>3</sup> and the EUROfusion MST1 Team[1]

<sup>1</sup> *Eindhoven University of Technology, Eindhoven, The Netherlands*

<sup>2</sup> *Department of Applied Physics, Ghent University, 9000 Ghent, Belgium*

<sup>3</sup> *Max-Planck-Institut für Plasmaphysik, Garching, Germany*

### Introduction

One of the challenges in fusion research is the optimisation of the operation regime of current and future tokamaks. An important figure of merit for plasma stability and performance is the safety factor ( $q$ ). It is inversely proportional to the current density and defined as the ratio of the number of  $m$  poloidal turns a field line has to complete to do  $n$  toroidal turns in the tokamak. However, no direct measurement of the full  $q$ -profile is available. It can be calculated by equilibrium reconstruction codes which solve the Grad-Shafranov equation ( $\equiv$  force balance in the plasma), constrained by polarisation angle measurements obtained by the Motional Stark Effect diagnostic (MSE). The MSE diagnostic measures the polarisation direction of light emitted by neutral particles injected into the plasma from which the local direction of the magnetic field can be derived. A challenge for the MSE diagnostic is the high accuracy required for equilibrium reconstruction, typically a few tenths of degrees. To enable MSE-constraint equilibrium reconstruction even in situations where high accuracy measurements are unavailable, such as the high-density discharges on the ASDEX-U tokamak (AUG) [2], we propose an observer-based approach to filter the measurements. An observer is based on a model of the system taking the underlying physics into account from which predictions about the expected measurement can be made. Combining the predicted and real measurement can generally lead to better results than would be obtainable by using only one of the two. As a model of our system, we use RAPTOR [3], a faster than real-time transport simulator which solves the coupled 1D poloidal flux diffusion and electron heat diffusion equations. From the poloidal flux  $\psi$  and electron temperature profile many otherwise unavailable parameters of the system can be reconstructed. We propose to use RAPTOR to filter the measured polarisation angles with an Extended Kalman Filter (EKF). The EKF has the advantage that it not only takes the measurement and model into account, but it is also recursive, fast and can handle asynchronous measurements.

## Implementation of Extended Kalman Filter

In this paragraph we will give a brief description of the EKF schema, shown in figure 1, after which the calculation of the predicted measurement is outlined in a more detail. For a complete description of the EKF algorithm, the interested reader is pointed towards [4]. The basis of the observer design is the predictive model, which simulates the state of the system. At time  $k$ , we thus not only have access to a measurement  $z_k$ , but also to the measurement prediction of the model,  $z_{k,\text{pred}} = h(\hat{x}_{k|k-1})$ . The subscript  $k|k-1$  denotes that the state  $x$  is taken at time  $k$  with information up to time  $k-1$ . An estimate of the state  $x$  at time  $k$  is made by updating the state prediction with the predicted and real measurement, like:  $\hat{x}_{k|k} = \hat{x}_{k|k-1} + L_k \cdot (z_k - z_{k,\text{pred}})$ , where,  $L_k(Q_k, R_k)$  is the Kalman Gain.  $L_k$  can in the simplest way be described as a weighting function, depending on the uncertainty of the state  $Q_k$  and the measurement  $R_k$ . The implementation of the EKF for the presented analysis follows [5] closely.

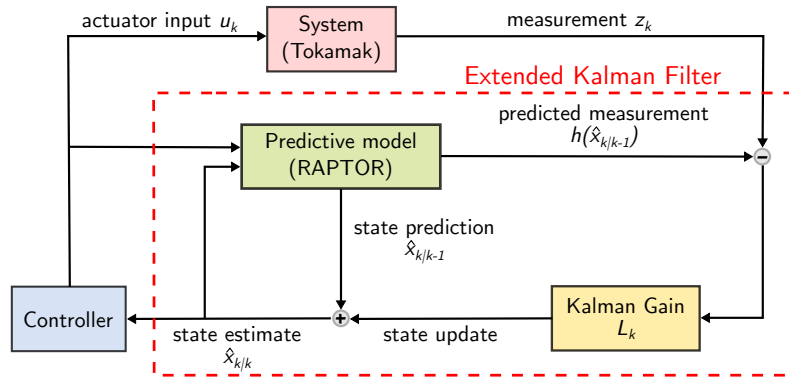


Figure 1: Overview of the Extended Kalman Filter: The predictive model (RAPTOR) simulates the state of the system from which the measurement (polarisation angle) can be predicted. In combination with the real measurement the state can be updated to obtain an improved estimate. Image after [6].

For the implementation of the EKF, the measurement (= the polarisation angle) must be calculated from the state of the model. The polarisation angle  $\gamma$  is calculated by:

$$\gamma = \tan^{-1} \left( \frac{a_0 B_z + a_1 B_r + a_2 B_t}{a_3 B_z + a_4 B_r + a_5 B_t} \right). \quad (1)$$

Here, the  $a_i$  are known geometric coefficients,  $B_z$  and  $B_r$  are the vertical and radial components of the poloidal magnetic field  $B_p$  and  $B_t$  is the toroidal magnetic field. The poloidal magnetic field can be expressed as

$$B_p = \mathbf{e}_t \times \nabla \psi = \mathbf{e}_t \times \left( R^{-1} \nabla \Phi \frac{\partial \psi}{\partial \Phi} \right) = \mathbf{e}_t \times (2\pi R)^{-1} \nabla \Phi q^{-1}, \quad (2)$$

where  $\mathbf{e}_t$  is the unit vector in the toroidal direction,  $R$  is the major radius,  $\psi$  is the poloidal

flux and  $\Phi$  is the toroidal flux. Combining the RHS of equation 2 and equation 1 we find:

$$\gamma = \tan^{-1} \left( \frac{-a_0 R \cdot \partial_R \Phi \cdot q^{-1} + a_1 R \cdot \partial_z \Phi \cdot q^{-1} + a_2 B_t}{-a_3 R \cdot \partial_R \Phi \cdot q^{-1} + a_4 R \cdot \partial_z \Phi \cdot q^{-1} + a_5 B_t} \right), \quad (3)$$

where  $\partial_j = \partial/\partial j$ . Clearly the polarisation angle cannot be calculated from RAPTOR alone as 2d information about the fields is required and RAPTOR solves the transport equation in 1d. For this reason we have rewritten the equation of the poloidal magnetic field as a function of the toroidal flux. The toroidal flux (and  $B_t$ ) can be obtained from an equilibrium solver. In our case we have coupled RAPTOR to CHEASE [7], a fixed-boundary equilibrium solver which reconstructs the plasma equilibrium with predefined profiles (here the  $q$ -profile and pressure profile from RAPTOR), by which a matching between  $\nabla\Phi$  and the  $q$ -profile is guaranteed. In a later implementation RAPTOR needs to be coupled to a free-boundary equilibrium reconstruction code such as JANET, where the matching of the  $q$ -profile between both codes can be implicitly guaranteed by passing the filtered polarisation angles as a constraint to the equilibrium solver.

### Simulation and Results

To evaluate the performance of the EKF we run a feedforward simulation with RAPTOR, initialised with equilibrium, heating and density profiles matching an AUG shot. The MSE diagnostic is simulated by calculating the expected polarisation angle measurement and adding a uniform random noise of  $\Delta\gamma = 0.5^\circ$ . Secondly,

the simulation is perturbed by the introduction of an artificial offset in the central  $q$ -profile and a reduction in electron temperature transport coefficient by a factor of  $\chi_{e,\text{red}} = 0.7 \cdot \chi_e$ . The feedforward (FF) and perturbed (PB)  $q$ -profiles at the beginning and end of the simulation are shown in figure 2. The perturbed  $q$ -profile, reduced transport coefficient and noised polarisation angles from the feedforward simulation are used to test the performance of the observer. The results are shown in figure 3. The model mismatch due to the reduced

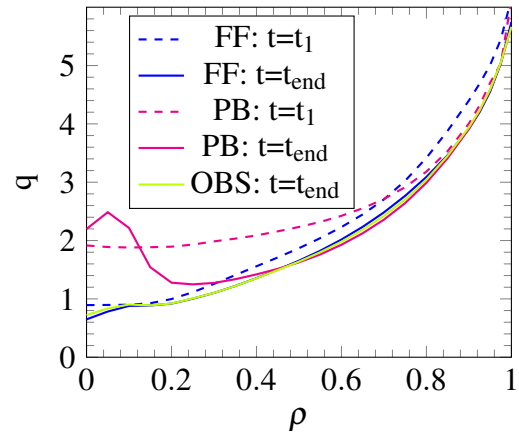


Figure 2:  $q$ -profiles of the feedforward (FF) and perturbed (PB) simulation as well as the filtered  $q$ -profile (OBS) at the end of the simulation ( $\Delta t_{\text{end}} = 500$ ).

transport coefficient can be seen in figure 3 (d), where the electron temperature evolution at different radii is plotted from the unperturbed (solid) and perturbed (dashed) simulation. Despite the model mismatch and difference in initial conditions, the  $q$ -profile (fig. 3 (b)) converges within a few tens of time steps to the state of the unperturbed simulation. The convergence time

depends strongly on the choice of the covariance matrix, which can be used to tune the EKF. The innovation sequence  $\mathcal{J} = z_k - h(\hat{x}_{k|k-1})$  (fig. 3(e)) converges to a zero mean once the initial offset in  $q$  has been corrected. Lastly we want to address the jumps in figure 3(b,c) (solid line), which result from the equilibrium update. Here a more careful implementation is required to avoid sudden changes in  $\nabla\Phi$ , for example by careful interpolation between equilibrium updates.

### Conclusion and Outlook

In this initial report it is shown how a simulated, high-noise polarisation angle measurement can be used to obtain an accurate  $q$ -profile reconstruction when a model mismatch is introduced. Using the EKF, a convergence with  $\overline{\Delta q} < 0.1$  (avg. over radius) was achieved in 50 time steps. For the future, a more careful implementation of the equilibrium update is required to achieve a smooth polarisation angle reconstruction in time. For future work a careful comparison between the RAPTOR simulations and reconstructed equilibria at AUG is required. This would allow to replace the plasma simulator CHEASE with an equilibrium solver and use real MSE measurements. If the EKF has been proven to work in an offline environment it could lastly be implemented in a real-time control system for active  $q$ -profile control.

**Acknowledgment** This work has been carried out within the framework of the EUROfusion Consortium and has received funding from the Euratom research

and training programme 2014-2018 under grant agreement No 633053. The views and opinions expressed herein do not necessarily reflect those of the European Commission.

### References

- [1] H. Meyer and E. al, *Nucl. Fusion FEC 2016 Spec. Issue*, 2017.
- [2] A. Bock, Ph.D. Thesis, Max-Planck-Institut für Plasmaphysik, Garching, 2016.
- [3] F. Felici, O. Sauter, S. Coda, B. Duval, T. Goodman, J.-M. Moret and J. Paley, *Nucl. Fusion*, 2011, **51**, 083052.
- [4] D. Simon, *Optimal State Estimation: Kalman and Nonlinear Approaches*, Wiley-Interscience, 2006.
- [5] F. Felici, M. D. Baar and M. Steinbuch, Am. Control Conf. 2014, pp. 4816–4823.
- [6] J. Loenen, Master Thesis, TU Eindhoven, 2016.
- [7] H. Lütjens, A. Bondeson and O. Sauter, *Comput. Phys. Commun.*, 1996, **97**, 219–260.

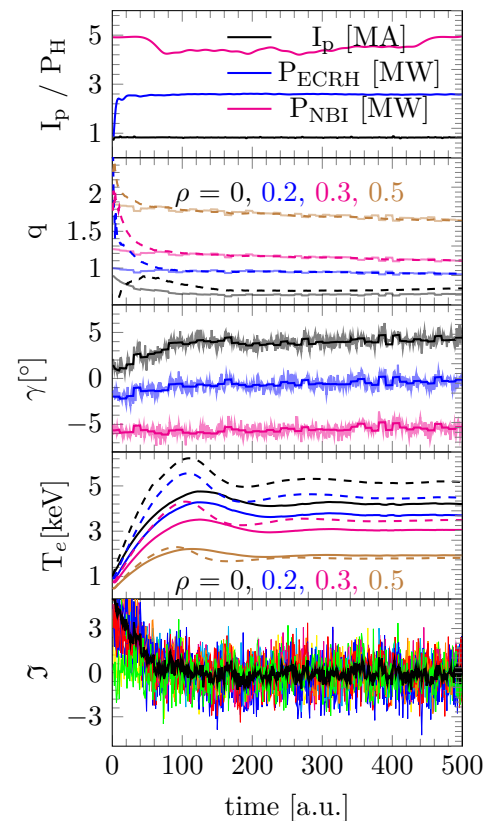


Figure 3: Profile comparison: Top to bottom: Plasma current and heating,  $q$ -profile at various  $\rho$ , (disturbed) polarisation angle (shaded), electron temperature and innovation sequence with mean in black.